

## A New Renal Mitochondrial Carrier, KMCP1, Is Up-regulated during Tubular Cell Regeneration and Induction of Antioxidant Enzymes\*

Received for publication, October 26, 2004, and in revised form, March 29, 2005  
Published, JBC Papers in Press, April 4, 2005, DOI 10.1074/jbc.M412136200

Anne Haguenaer‡, Serge Raimbault†‡, Sandrine Masscheleyn‡,  
Maria del Mar Gonzalez-Barroso‡, Francois Criscuolo‡, Julie Plamondon§, Bruno Miroux‡,  
Daniel Ricquier‡, Denis Richard§, Frederic Bouillaud‡, and Claire Pecqueur†¶

From ‡CNRS UPR9078, Faculté Necker-Enfants Malades, 156 Rue de Vaugirard, 75730 Paris Cedex 15, France and the §Département d'Anatomie et de Physiologie, Faculté de Médecine, Université Laval, Québec G1K 7P4, Canada

**The mitochondrial carrier family transports a variety of metabolites across the inner mitochondrial membrane. We identified and cloned a new member of this family, KMCP1 (kidney mitochondrial carrier protein-1), that is highly homologous to the previously identified protein BMCP1 (brain mitochondrial carrier protein-1). Western blotting and *in situ* experiments showed that this carrier is expressed predominantly within the kidney cortex in the proximal and distal tubules. KMCP1 was increased during fasting and during the regenerative phase of glycerol-induced renal failure. We show that both situations are associated with transiently increased expression of superoxide-generating enzymes, followed by increased mitochondrial metabolism and antioxidant defenses. Given that KMCP1 expression occurs simultaneously with these latter events, we propose that KMCP1 is involved in situations in which mitochondrial metabolism is increased, in particular when the cellular redox balance tends toward a pro-oxidant status.**

The main function of mitochondria is to create energy for cellular activity by the process of oxidative phosphorylation. Mitochondria are also critical for other aspects of cell function such as modulation of calcium storage, heme biosynthesis, and apoptosis. Mitochondrial dysfunction, generally arising from oxidative damage or mutation to mitochondrial or nuclear genes, contributes to a wide range of human diseases, including neurodegenerative diseases and diabetes. Oxidative stress is a particularly important factor in mitochondrial metabolism; the respiratory chain continually produces free radical superoxide, leading to mitochondrial dysfunction, cell damage, and death by compromising ATP production and increasing oxidative stress. All of these mitochondrially mediated processes require exchange of solutes between the mitochondrial matrix and the cytoplasm. Although the outer mitochondrial membrane is permeable to many small metabolites, transport of solutes across

the inner mitochondrial membrane is achieved by members of the mitochondrial carrier protein family (or SLC25 family) (1). These proteins share a structure containing three domains repeated in tandem, each containing a conserved motif and folded into two transmembrane domains connected by a hydrophilic loop, (2). The substrates transported by these carriers vary widely in their structure and size from the smallest, H<sup>+</sup>, to the largest and most highly charged species, ATP. Some mitochondrial carriers are present in all tissues, whereas others are tissue-specific and have a limited distribution reflecting their importance in special functions. Functional studies in intact mitochondria have indicated the presence of ~20 carriers for the transport of metabolites involved in oxidative phosphorylation; the citric acid cycle; fatty acid oxidation; gluconeogenesis; lipogenesis; transfer of reducing equivalents; urea synthesis; amino acid degradation; and intramitochondrial DNA, RNA, and protein synthesis.

In this study, we identify a new mitochondrial carrier, KMCP1 (kidney mitochondrial carrier protein-1), that is expressed mainly in the kidney and that is highly similar to BMCP1 (brain mitochondrial carrier protein-1), a mitochondrial carrier expressed mainly in the brain (3–7) and potentially involved in metabolic status such as starvation or ketogenic diet (6–10). We examine a number of models of kidney injury and show that KMCP1 expression is up-regulated in response to increased energy demands associated with cellular oxidative damage.

### EXPERIMENTAL PROCEDURES

**Chemicals, Media, and Antibodies**—Protease inhibitors, CAPS,<sup>1</sup> Tween 20, the bicinchoninic acid kit, insulin transferrin selenium, triiodothyronine, hydroxyquinolol, ferrous ammonium sulfate, dexamethasone, horseradish peroxidase-conjugated rabbit and mouse antibodies, anti-cyclooxygenase-2 antibodies, and purified oligonucleotides were purchased from Sigma. Anti-heme oxygenase-1 antibody was purchased from Stressgen Biotech Corp. Polyclonal antibodies against caspase-3 and proliferating cell nuclear antigen (PCNA) were purchased from tebu-bio. Enzymes were obtained from New England Biolabs Inc. The ECL detection kit and [ $\alpha$ -<sup>32</sup>P]dCTP were purchased from Amersham Biosciences. Culture media, fetal calf serum, TRIzol reagent, Lipofectamine 2000, epidermal growth factor, and Moloney murine leukemia virus reverse transcriptase were obtained from Invitrogen. HK2 cells were kindly provided by Dr. Corinne Antignac and the carnitine palmitoyltransferase-1 probe was from Dr. Karina Prib-Buus. Urea kinetic and creatinine kinetic kits were purchased from bioMérieux.

**Animals and Treatments**—C57BL/6J mice (6–8 weeks old) were

\* This work was supported by CNRS and by European Community Sixth Framework Program Contract LSHM-CT-2003-503041. The costs of publication of this article were defrayed in part by the payment of page charges. This article must therefore be hereby marked "advertisement" in accordance with 18 U.S.C. Section 1734 solely to indicate this fact.

This paper is dedicated to the memory of Serge Raimbault.

The nucleotide sequence(s) reported in this paper has been submitted to the GenBank™/EBI Data Bank with accession number(s) NM\_026232 and NM\_001010875.

† Deceased.

¶ To whom correspondence should be addressed. Tel.: 33-1-4061-5697; Fax: 33-1-4061-5673; E-mail: pecqueur@necker.fr.

<sup>1</sup> The abbreviations used are: CAPS, 3-(cyclohexylamino)propanesulfonic acid; PCNA, proliferating cell nuclear antigen; TUNEL, terminal deoxynucleotidyltransferase-mediated dUTP nick end labeling; RACE, rapid amplification of cDNA ends; GFP, green fluorescent protein; contig, group of overlapping clones.

obtained from Elevage Janvier (Le Genest Saint Isle, France) and maintained under normal conditions with free access to food and water. On the day of the experiment, mice were injected intramuscularly with a 50% glycerol solution (10 ml/kg), gentamicin (100 mg/kg/d), or cyclosporin A (5 mg/kg/d). Furosemide (400 mg/kg), acetazolamide (200 mg/kg), hydrochlorothiazide (200 mg/kg), and acetylcysteine (15 mg/kg) were injected intraperitoneally as indicated. For diet assays, mice were fed a 0.01% NaCl, 3% NaCl, or 3% KCl diet for 1 week. For starvation assays, mice were deprived of food for 8–36 h. Metabolic acidosis was induced by addition of 0.28 M  $\text{NH}_4\text{Cl}$  to the water for 48 h. For all treatments (except diuretic treatment, which lasted 5 h), mice were killed by cervical dislocation 3 days after injection, and tissues were removed immediately. One kidney was frozen in liquid nitrogen for RNA and mitochondrial extraction, and the other was processed for histological examination. Blood samples for serum creatinine and urea measurements were taken. In general, experiments included at least four mice in two independent experiments.

**Immunohistology Assays**—Mice kidneys were placed overnight in phosphate-buffered saline containing 4% paraformaldehyde at 4 °C and then embedded in paraffin. Serial kidney sections (6  $\mu\text{m}$ ) were deparaffinized, stained with hematoxylin/eosin, and assayed for *in situ* hybridization or apoptosis detection with the TUNEL method according to the instructions of Roche Diagnostics.

**Cloning of Mouse KMCP1 cDNA**—KMCP1 cDNA was obtained by reverse transcription-PCR from mouse kidney RNA (oligonucleotides 5'-CAGACAAATGATGCCAACTTCC (forward) and 5'-AGCAAAAAC-CCTTCATTCTTCC (reverse)) and then subcloned into the pCRII vector using a TOPO TA cloning kit (Invitrogen) according to the manufacturer's instructions. After transformation of electrocompetent bacteria (JM109), the construct was verified by sequencing.

**5'-RACE Analysis**—Determination of the beginning of transcription was performed using a GeneRacer 5'-RACE kit (Invitrogen) according to the manufacturer's instructions with mouse kidney poly(A)<sup>+</sup> mRNA as template (PolyATtract mRNA isolation system II, Promega Corp.).

**Purification of KMCP1 and Production of anti-KMCP1 Antibodies**—Mouse full-length KMCP1 was produced as inclusion bodies in *Escherichia coli* strain C41(DE3) and purified as described previously (11, 12). Purified protein was sent to Elevage Scientifique des Dombes (Lyon, France) for rabbit immunization. Rabbit sera were precipitated with ammonium sulfate as described (13) and purified by affinity chromatography on a KMCP1-N-hydroxysuccinimide column (Amersham Biosciences). Antibodies were tested, and the most specific one was chosen for the following analysis.

**Immunoprecipitation Experiments**—For immunoprecipitation experiments, mitochondrial proteins were solubilized overnight with immunoprecipitation buffer (150 mM NaCl, 1% Nonidet P-40, 0.1% SDS, and 50 mM Tris (pH 7.5)) at 4 °C and centrifuged at 20,000  $\times g$  for 30 min. Anti-KMCP1 antibody was added to the supernatant for 2 h at room temperature. Immunoprecipitated proteins were retrieved by addition of protein A and analyzed by Western blotting.

**Cell Culture**—The simian kidney epithelial cell line COS-7 was maintained in Dulbecco's modified Eagle's medium supplemented with 10% fetal calf serum, 100 units of penicillin, and 50  $\mu\text{g}$  of streptomycin. Cells were transiently transfected with Lipofectamine 2000 according to the manufacturer's instructions and harvested 24 h after transfection. HK2 cells were maintained in 50% Dulbecco's modified Eagle's medium and 50% Ham's F-12 medium supplemented with antibiotics, insulin, transferrin, selenium, triiodothyronine (4 pg/ml), dexamethasone (0.5 nM), fetal calf serum (1%), and epidermal growth factor (10 ng/ml). When near confluence, cells were exposed to an equimolar solution of hydroxyquinolol/ferrous ammonium sulfate, 0.1  $\mu\text{M}$  prostaglandin I<sub>2</sub>, or 0.1  $\mu\text{M}$  angiotensin II. For cell starvation experiments, the cell medium was replaced with a nutrient-poor medium. Cells were harvested in Tris/sucrose buffer (10 mM Tris and 250 mM sucrose (pH 7.4) containing protease inhibitors and DNase), frozen in liquid nitrogen for 5 min, and incubated at 37 °C for 10 min. These steps were repeated twice. Unbroken cells were removed by centrifugation at 750  $\times g$  for 10 min. Mitochondria were collected after centrifugation of the supernatant at 10,000  $\times g$  for 20 min. The pellet was resuspended in Tris/sucrose buffer.

**RNA Analysis**—Total RNA from mouse tissue was prepared using TRIzol reagent. Northern analysis of 20  $\mu\text{g}$  of total tissue RNA was performed using a [ $\alpha$ -<sup>32</sup>P]dCTP-labeled KMCP1 cDNA probe as described previously (14). A [ $\alpha$ -<sup>32</sup>P]dCTP-labeled R45 rRNA probe was used as standard. Quantification was achieved with a PhosphorImager. Reverse transcription PCR was performed with 2  $\mu\text{g}$  of mouse mRNA using Moloney murine leukemia virus reverse transcriptase according to the manufacturer's instructions. Real-time PCR was performed on a

LightCycler instrument with 1  $\mu\text{l}$  of the reverse transcription product and LightCycler FastStart DNA Master SYBR Green mixture (oligonucleotides 5'-TGCTGCACGCGCTGATGAGGATAGG (forward) and 5'-T-GGAAGCTCCACGCCGACCACAATG (reverse)). For *in situ* hybridization, brain and kidney sections were hybridized with mouse KMCP1 cDNA sense and antisense probes.

**Protein Analysis**—Mitochondrial proteins were isolated from mouse tissues as described previously (11). Mitochondrial protein content was assayed by the bicinchoninic acid method. Protein were loaded onto a 10% SDS-polyacrylamide gel and transferred to nitrocellulose membrane by liquid electroblotting in 10 mM CAPS and 10% ethanol (pH 9). Nonspecific binding was achieved at room temperature in phosphate-buffered saline and Tween 20 supplemented with 5% dried milk for 1 h. All antibodies were diluted in phosphate-buffered saline, Tween 20, and 2% dried milk and incubated overnight at 4 °C. The appropriate peroxidase-conjugated antibody was used to reveal protein binding with an ECL kit. Quantification was achieved using Syngene GeneSnap software (Ozyme, Saint Quentin en Yvelines, France). All membranes were probed with anti-porin monoclonal antibody (Molecular Probes, Inc.) to normalize protein loading. COS-7 cells transiently transfected with KMCP1 were used as a positive control.

**Mitochondrial Respiration Analysis in Yeast**—The yeast expression vector pYeDP containing the protein of interest was used to transform yeast strain IB111. Yeast growth rate was determined as described (15), and proton leak measurements were obtained as described (16). Briefly, yeast mitochondria were isolated and resuspended in 0.65 M mannitol, 10 mM Tris maleate, 0.5 mM EGTA, 2 mM  $\text{MgCl}_2$ , 10 mM phosphate, and 0.1% bovine serum albumin (pH 6.8). Oxygen consumption and membrane potential were measured simultaneously in an Oxygraph chamber (Hansatech Instruments) in the presence of 3 mM NADH, 1  $\mu\text{g/ml}$  oligomycin, and 100 ng/ml nigericin. The proton conductance of yeast was determined by measuring the oxygen consumption relative to the mitochondrial membrane potential (3). All experiments were performed using two other members of the mitochondrial carrier family, UCP1 (uncoupling protein-1) and the oxoglutarate carrier, as internal controls.

**Mitochondrial Membrane Potential Analysis in COS-7 Cells**—KMCP1, oxoglutarate carrier, and UCP1 cDNAs were cloned into the pTracer-CMV vector (Invitrogen) containing an SV40 promoter driving expression of a green fluorescent protein (GFP) gene and the cytomegalovirus promoter driving expression of the protein of interest. Transiently transfected COS-7 cells were harvested by trypsinization and incubated for 30 min at 37 °C with the red fluorescent probe tetramethylrhodamine ethyl ester (100 nM; Molecular Probes, Inc.) with or without 10 nM oligomycin. Flow cytometry analysis allowed the identification of transfected cells by measuring green fluorescence, whereas membrane potential was determined by measuring red fluorescence. The ratio between transfected cells and non-transfected fluorescent cells was calculated and is expressed relative to control pTracer vector-transfected cells.

**Superoxide Dismutase Activity Analysis**—Mouse kidneys were homogenized in 10 mM Tris (pH 7.5), 1 mM EDTA, and 250 mM sucrose and solubilized with addition of 0.1% of Triton X-100 at 4 °C. Basal pyrogallol autooxidation was measured at 37 °C at 420 nm by spectrophotometry in 0.1 M Tris/cacodylic acid buffer (pH 8.5), 2 mM pyrogallol, 1.7 mM diethylenetriaminepentaacetic acid (pH 7) (Sigma). Superoxide dismutase activity inhibits this oxidation. Result are presented as the inverse of the ratio between autooxidation of pyrogallol and its oxidation in the presence of kidney lysate.

**Statistical Analysis**—Data are expressed as means  $\pm$  S.E. Comparison between groups was made using one-way analysis of variance. Differences were considered as significant if  $p < 0.05$ .

## RESULTS

**Identification of a Novel Mitochondrial Carrier Family Member, KMCP1**—To identify novel mitochondrial carrier family members, an *in silico* search was performed in UniGene (available at [www.ncbi.nlm.nih.gov](http://www.ncbi.nlm.nih.gov)). A set of expressed sequence tags, mostly from adult mouse kidney, were found. They were similar but not identical to mouse and human BMCP1 (GenBank<sup>TM</sup> accession numbers BB609460, BB610721, BB619998, BB853686, BF786152, and B1691726). Primers designed based on a contig construction sequence using these expressed sequence tags were used to clone a mouse cDNA and a human cDNA (GenBank<sup>TM</sup> accession numbers NM\_026232 and NM\_001010875, respectively) termed KMCP1 (SLC25A30). The full-length cDNA was generated as described under "Ex-

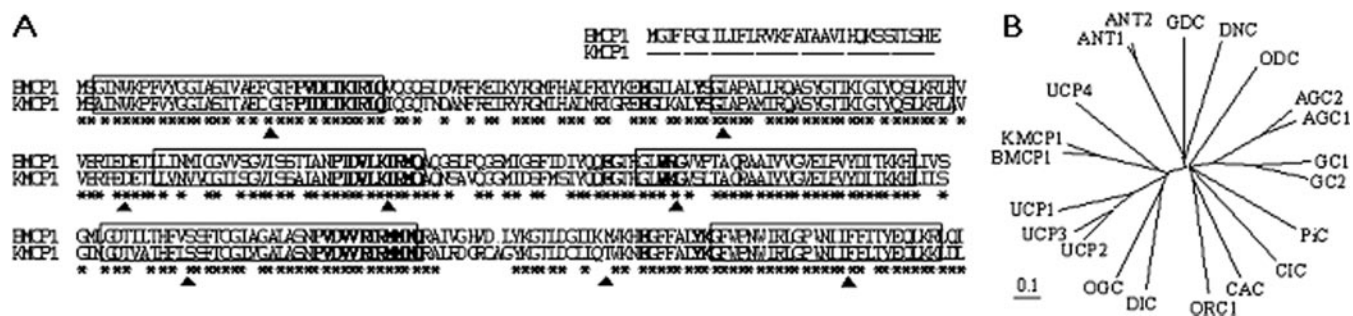


FIG. 1. **KMCP1, a new mitochondrial carrier.** A, sequence alignment of the mouse BMCP1 and KMCP1 proteins shows the three repeats of 100 amino acids. Asterisks indicate identical amino acids between the two proteins. Boldface letters indicate consensus mitochondrial carrier motifs (PROSITE PS00215 and the EGXXXXKG motif). Transmembrane helices are boxed (2, 27). Amino acids adjacent to splice sites are indicated ( $\blacktriangle$ ). B, the phylogenetic tree of the known mouse mitochondrial carriers shows that KMCP1 is closer to BMCP1 than to any of the other mitochondrial carrier proteins. This tree was generated from alignment using the ClustalW program. The bar indicates the number of substitutions/residue, with 0.1 corresponding to a distance of 10 substitutions/100 residues. ANT, adenine-nucleotide translocase; GDC, Graves disease carrier; DNC, deoxynucleotide carrier; ODC, oxodicarboxylate carrier; AGC, aspartate/glutamate carrier; GC, glutamate carrier; PiC, phosphate carrier; CIC, citrate carrier; CAC, carnithine/acylcarnithine carrier; ORC, ornithine carrier; DIC, dicarboxylate carrier; OGC, oxoglutarate carrier.

perimental Procedures." KMCP1 is a 291-amino acid protein with a theoretical molecular mass of 32,245 Da. Alignment of its predicted sequence with BMCP1 showed a strong homology (Fig. 1A). In fact, if the N-terminal 20 amino acids present uniquely in BMCP1 are not included in analysis, these proteins share 80% identity. The relationship to other mitochondrial carrier proteins is shown in Fig. 1B. As in all mitochondrial carrier family members, the protein sequence displays both the 3-fold repeat structure of 100 amino acids and the characteristic mitochondrial motifs (Fig. 1A). The human gene maps to chromosome 13q14.11. To our knowledge, this locus is not genetically linked to any pathophysiological situation. The intron/exon structure of the mouse gene consists of 10 exons (Fig. 1A). The first exon is untranslated because the ATG site is located within the second exon. Exon 10 contains a TGA codon followed by a polyadenylation site and a very long untranslated region (2655 bp).

**KMCP1, a Mitochondrial Kidney Protein**—Northern blot analysis of KMCP1 RNA expression in murine tissues revealed that KMCP1 was expressed as a 3.7-kb mRNA transcript mainly in the kidney and at lower levels in the testes and white adipose tissue (Fig. 2A). A weak signal was detected in other tissues. A polyclonal antibody was made against the recombinant mouse full-length KMCP1 protein expressed in *E. coli* as described under "Experimental Procedures." Its specificity against KMCP1 compared with both BMCP1 and other members of the mitochondrial carrier family was tested by Western blot analysis (Fig. 2B). Anti-KMCP1 antibody detected 5 ng of KMCP1 inclusion bodies extracted from recombinant bacteria. This antibody detected the same amount of BMCP1, but barely detected other mitochondrial carriers such as UCP1, UCP2, and UCP3. The KMCP1 protein was also revealed by Western blotting in COS-7 cells transiently transfected with a mammalian expression vector overexpressing KMCP1 (Fig. 2C). Western blot analysis was performed using mitochondria from various tissues. Anti-KMCP1 antibody revealed a 30-kDa protein in kidney lysate that comigrated with KMCP1 overexpressed in COS-7 cells (Fig. 2D). However, another band at a slightly higher molecular mass appeared in spleen and testis mitochondria (Fig. 2D), suggesting that the antibody cross-reacts with other proteins. To test this hypothesis, immunoprecipitation experiments were performed. Although immunoprecipitation of spleen mitochondria followed by Western blotting did not reveal any band, immunoprecipitation of kidney mitochondria revealed the same 30-kDa band (Fig. 2E). This 30-kDa band immunoprecipitated from kidney mitochondria comigrated with KMCP1 immunoprecipitated from yeast expressing KMCP1. Finally, to confirm the mitochondrial localization of

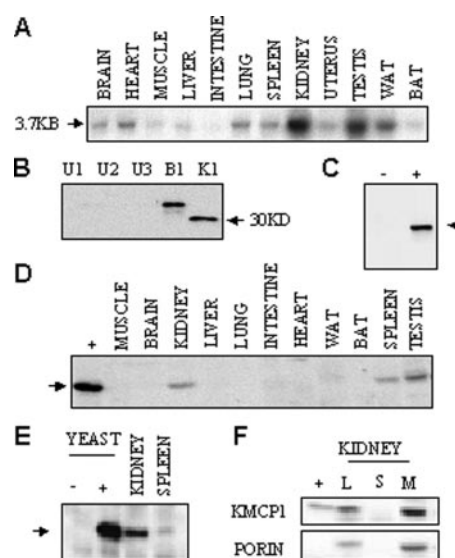
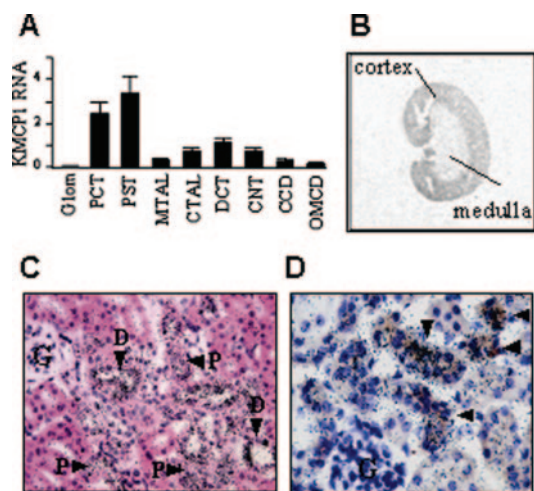


FIG. 2. **Tissue distribution of KMCP1 in mice.** A, shown is KMCP1 RNA expression. Northern blotting was performed with total RNA (20  $\mu$ g) isolated from various mouse tissues using  $^{32}$ P-labeled mouse KMCP1 cDNA. WAT, white adipose tissue; BAT, brown adipose tissue. B, inclusions bodies from *E. coli* overexpressing UCP1 (U1), UCP2 (U2), UCP3 (U3), BMCP1 (B1), and KMCP1 (K1) were loaded onto a 11% SDS-polyacrylamide gel and analyzed by Western blotting with antibody raised against the mouse full-length KMCP1 protein (this study). C, mitochondria were isolated from COS-7 cells transiently transfected with control vector (-) and KMCP1 (+). KMCP1 was detected by Western blotting with anti-KMCP1 antibody. D, mitochondria from various mouse tissues were loaded onto a 11% SDS-polyacrylamide gel. Western blot analysis was performed using anti-KMCP1 antibody. Mitochondria isolated from COS-7 cells transiently overexpressing KMCP1 were used as a positive control (+). E, the KMCP1 protein was immunoprecipitated from control yeast (-) and yeast expressing KMCP1 (+) as well as from kidney and spleen mitochondria using anti-KMCP1 antibody. Immunoprecipitated proteins were revealed by Western blot analysis as described for B. F, 15  $\mu$ g of lysate (L), 10,000  $\times$  g supernatant (S), and mitochondria (M) were loaded onto 10% SDS-polyacrylamide gel. COS-7 cells transiently overexpressing KMCP1 were used as a positive control (+). Western blot analysis was performed with anti-KMCP1 antibody (K1) and with anti-porin for mitochondrial enrichment.

this protein, Western blot analysis was performed with lysate, a 10,000  $\times$  g supernatant, and mitochondria prepared from mouse kidney. The weak band detected in kidney lysate was strongly enhanced by mitochondrial enrichment (Fig. 2F). No signal was detected in the 10,000  $\times$  g supernatant. Thus, KMCP1 is a mitochondrial protein expressed mainly in the kidney.



**FIG. 3. Sublocalization of KMCP1 in the kidney.** *A*, quantitative real-time PCR analysis realized with microdissected nephron segment parts: glomerulus (*Glom*), proximal convoluted tubule (*PCT*), proximal straight tubule (*PST*), medullary thick ascending limb (*MTAL*), cortical thick ascending limb (*CTAL*), distal convoluted tubule (*DCT*), connecting tubule (*CNT*), cortical collecting tubule (*CCD*), and outer medulla collecting tubule (*OMCD*) ( $n = 6$ ). *B*, *in situ* hybridization with kidney sections using the mouse KMCP1 cDNA antisense probe (magnification  $\times 40$ ). *C*, *in situ* hybridization with kidney cortex sections using the mouse KMCP1 cDNA antisense probe. Positive cells (silver grains) in distal tubule (*D*) and proximal tubule (*P*) are indicated by arrowheads (magnification  $\times 400$ ). Sections were stained with hematoxylin and eosin. Glomeruli are indicated (*G*). *D*, immunohistochemistry with kidney cortex sections using anti-KMCP1 antibody, followed by *in situ* hybridization experiments using the mouse KMCP1 cDNA antisense probe (magnification  $\times 400$ ). Brown peroxidase staining revealed KMCP1 protein colocalized with KMCP1 RNA as indicated by the arrowheads. Sections were stained with hematoxylin only. Glomeruli are indicated (*G*).

**Sublocalization of KMCP1 in the Kidney**—To determine more precisely the localization of KMCP1 within the kidney, real-time PCR was performed using mRNA from microdissected nephron segments as described previously (17). KMCP1 RNA seemed to be predominantly expressed in proximal tubules, although a fair amount of expression was also detected in distal tubules and surrounding nephron segments (Fig. 3A). KMCP1 RNA was barely detected in glomeruli, the medullary part of the loop of Henle, and the collecting duct. *In situ* hybridization showed that KMCP1 RNA was clearly restricted to the renal cortex (Fig. 3B). These experiments confirmed a low level of KMCP1 RNA in the glomeruli and collecting ducts, with higher levels in the proximal and distal tubules. However, KMCP1 expression was as abundant in the distal tubules as in the proximal tubules (Fig. 3C). No staining was observed with a KMCP1 cDNA sense probe (data not shown). Finally, immunohistochemistry using anti-KMCP1 antibody followed by KMCP1 *in situ* hybridization within kidney cortex sections showed colocalization of staining between RNA and protein in tubular cells (Fig. 3D).

**Physiological Challenges and KMCP1 Expression**—To understand the physiological relevance of KMCP1 in the kidney, KMCP1 expression levels were recorded in response to several well characterized models of perturbed renal function (Table I). Although a number of these physiological perturbances did not induce any change in KMCP1 expression, we found that a potassium-rich diet, fasting, and some of the drug-induced acute renal failure models significantly increased KMCP1 expression (Table I).

**KMCP1 Expression during Glycerol-mediated Acute Renal Failure**—Because KMCP1 RNA levels increased nearly 2-fold after glycerol injection (Table I), we chose to investigate this model of renal failure in a more detailed manner. Serum blood

urea nitrogen and serum creatinine levels were measured, and histological examination of mouse kidney was performed before and 3 h and 1, 2, and 3 days after glycerol injection. Both blood urea nitrogen and serum creatinine levels increased 3 h after glycerol injection ( $13.7 \pm 0.1$  versus  $5.1 \pm 0.2$  mmol/liter and  $317 \pm 37$  versus  $150 \pm 19$  mmol/liter, respectively;  $p < 0.01$ ). During the following days, although creatinine levels progressively decreased to basal levels ( $164 \pm 28$  and  $160 \pm 16$  mmol/liter on days 2 and 3, respectively), blood urea nitrogen levels still increased and reached a maximum on days 2 and 3 ( $46.8 \pm 14$  mmol/liter ( $p < 0.001$ ) and  $38.2 \pm 11$  mmol/liter ( $p < 0.01$ ), respectively). Morphological changes were observed primarily in proximal tubules in the renal cortex. Although the basal membranes of tubules generally remained intact, most of them showed apical brush-border loss as early as 3 h after glycerol injection (Fig. 4A, upper right panel). In a few glomeruli, there was swelling of the mesangial space; however, most of them appeared to be normal. One day following glycerol injection, many of the proximal tubules showed cell vacuolization, detachment of epithelial cells, and necrosis (Fig. 4A, lower left panel). Changes in distal tubule cell morphology were also observed, with epithelial cell flattening and tubule dilatation (Fig. 4A, lower right panel). On days 2 and 3 after glycerol injection, the renal cortex showed a mixture of tubules that had undergone complete necrosis and tubules that had undergone tubular cell regeneration (Fig. 4A, lower right panel).

Apoptosis was estimated by performing Western blotting using anti-caspase-3 antibody as well as TUNEL experiments. Caspase-3 levels increased progressively during the days following glycerol injection and reached a maximum on day 3 ( $2.8 \pm 0.4$ -fold compared with control;  $p < 0.001$ ) (Fig. 4B). TUNEL experiments conducted at 3 h and 3 days in the kidney as early as 3 h after glycerol injection (data not shown). No change in the RNA levels of KMCP1 was observed 3 h following the insult (Fig. 4B). However, its expression increased 2–3-fold by days 2 and 3 both at the RNA ( $p < 0.001$ ) and protein ( $p < 0.001$ ) levels (Fig. 4B). *In situ* hybridization showed that KMCP1 RNA was strongly and specifically increased in proximal tubules on days 2 and 3 after glycerol injection (Fig. 4C). Interestingly, although KMCP1 expression did not change in tubules undergoing necrosis, it was highly up-regulated in regenerating tubules (Fig. 4C). In fact, cell proliferation as evidenced by PCNA followed the same time course as KMCP1, with increased levels of PCNA expression observed on days 2 and 3 (Fig. 4B). Cell differentiation as shown by vimentin levels began on day 3 (Fig. 4B). In addition, the level of carnitine palmitoyltransferase-1 increased progressively during the time course experiment (Fig. 4B) to reach a plateau on day 2. Because carnitine palmitoyltransferase-1 regulates entry of long-chain fatty acids into mitochondria, where they undergo  $\beta$ -oxidation, its level reflects mitochondrial lipid metabolism. Thus, the highest level of KMCP1 expression concurs with the highest degree of mitochondrial lipid oxidation. These results suggest that increased KMCP1 expression is associated with increased mitochondrial metabolism.

**Glycerol-mediated Nephrotoxicity Promotes Oxidative Stress**—Because a previous study (18) suggested that glycerol injection causes renal failure due to oxidative stress, we measured the expression pattern of heme oxygenase-1 and cyclooxygenase-2, which are involved in the generation of superoxide. We also measured superoxide dismutase activity, which is known to be up-regulated in response to oxidative stress. Expression of heme oxygenase-1 was strongly and transiently increased on day 1 after glycerol injection, and expression of cyclooxygenase-2 increased on days 2 and 3 ( $p < 0.05$ ) (Fig. 5A). Both

TABLE I  
KMCP1 RNA variations in various physiological challenges

	KMCP1 RNA variation <sup>a</sup>	n <sup>b</sup>	p value <sup>c</sup>
<b>Diet</b>			
Water deprivation for 12 h	0.73 ± 0.13	2	NS <sup>d</sup>
Hyponatremic diet (0.01% NaCl)	1.13 ± 0.25	3	NS
Hypernatremic diet (3% NaCl)	1.16 ± 0.12	5	NS
Hyperkalemic diet (3% KCl)	1.85 ± 0.36	5	p<0.001
18-h fasting	1.92 ± 0.07	11	p<0.001
<b>Diuretics</b>			
Furosemide (i.p., 400 mg/kg, 5 h)	0.66 ± 0.08	4	NS
Acetazolamide (i.p., 200 mg/kg, 5 h)	1.18 ± 0.01	2	NS
Hydrochlorothiazide (i.p., 200 mg/kg, 5 h)	1.30 ± 0.16	2	NS
<b>Induced nephrotoxicity</b>			
Metabolic acidosis (NH <sub>4</sub> Cl in water, 48 h)	1.07 ± 0.10	4	NS
Cyclosporin A (i.m., 5 mg/kg/d, 3 days)	1.11 ± 0.21	2	NS
Acetyl cysteine (i.p., 15 mg/kg)	1.29 ± 0.06	2	NS
Glycerol (i.m., 10 ml/kg of 50%, 3 days)	1.81 ± 0.13	17	p<0.001
Gentamicin (i.m., 100 mg/kg/d, 3 days)	1.48 ± 0.10	10	p<0.05
Cisplatin (i.p., 20 mg/kg, 3 days)	1.75 ± 0.11	3	p<0.05

<sup>a</sup> KMCP1 RNA variations analyzed by Northern blotting are presented as means ± S.E.M.

<sup>b</sup> n is the number of mice in each group.

<sup>c</sup> p values were calculated *versus* the control using, one-way analysis of variance.

<sup>d</sup> NS, not significant; i.p., intraperitoneally; i.m., intramuscularly.

cytoplasmic and mitochondrial superoxide dismutase activities were increased from day 1 to day 3 (Fig. 5B).

It has also been postulated that glycerol injection promotes iron release from heme (18), resulting in free radical formation. To determine whether iron could induce KMCP1 expression in this model, we investigated the effect of iron *in vitro* on KMCP1 levels in a human renal cell line endogenously expressing KMCP1 (HK2 cells) (Fig. 5C). KMCP1 protein expression was increased 2-fold after addition of 4 μM iron to the cell medium for 24 h. At a higher iron concentration (15 μM), only 4 h of treatment were sufficient to increase KMCP1 expression.

**KMCP1 and Mitochondrial Uncoupling**—One potential explanation for KMCP1 up-regulation in response to oxidative stress is an ability to uncouple mitochondrial respiration from ATP synthesis. Other mitochondrial carriers such as UCP1, UCP2, and UCP3 and even BMCP1 have been shown to have varying degrees of uncoupling activity. We set out to determine whether KMCP1 has any uncoupling activity in both yeast and mammalian systems. The growth rate of yeast remained unchanged upon induction of KMCP1 expression relative to the control vector (175 ± 3 *versus* 172 ± 6, respectively). As expected, the oxoglutarate carrier displayed no uncoupling activity, whereas expression of UCP1 in yeast led to an increase in proton conductance for the same membrane potential value (Fig. 6A). KMCP1 expression did not lead to a significant change in proton leaking compared with the oxoglutarate carrier (Fig. 6A).

To confirm the results obtained in yeast, we established a system in which cells were transiently transfected with vectors expressing both GFP and KMCP1, UCP1, or the oxoglutarate carrier. Flow cytometry analysis was then performed using GFP fluorescence to select cells expressing one of the mitochondrial carriers and the red fluorescent tetramethylrhodamine ethyl ester probe to monitor the mitochondrial membrane potential. Again, compared with COS-7 cells expressing the oxoglutarate carrier, COS-7 cells expressing UCP1 showed a significantly decreased membrane potential (Fig. 6B). In contrast, COS-7 cells expressing KMCP1 exhibited the same membrane potential as COS-7 cells expressing the oxoglutarate carrier (Fig. 6B). Addition of oligomycin, which hyperpolarizes mitochondria, did not enhance the difference between KMCP1- and oxoglutarate carrier-expressing cells. Similar experiments performed in HK2 cells led to the same results (data not shown). Taken together, these data argue against a respiration-uncoupling activity of KMCP1.

**KMCP1 Expression and Fasting**—KMCP1 expression was also up-regulated in response to fasting. Both RNA and protein levels increased 2-fold at 18 h of fasting (1.9 ± 0.07 (*p* < 0.001) and 2 ± 0.2 (*p* < 0.01), respectively) and decreased to almost control levels after 30 h of fasting (Fig. 7A). To identify similar cellular pathways in the kidney during both glycerol-mediated renal failure and fasting, similar protein measurements were performed. Western blot analysis of heme oxygenase-1 and caspase-3 proteins did not show any variation in protein levels (data not shown). However, the cyclooxygenase-2 protein was strongly increased after 8 h of fasting (Fig. 7A). Its level gradually returned to its approximate base-line level within 18 h. The activity of the mitochondrial superoxide dismutase significantly increased from 8 to 18 h of starvation (Fig. 7B). *In situ* hybridization showed that KMCP1 expression was induced in both proximal and distal tubular cells in response to fasting (Fig. 7C). However, although KMCP1 induction with the glycerol challenge was very strong and cell-specific, KMCP1 induction during fasting seemed more widespread. During fasting, creatinine values did not change significantly, but blood urea nitrogen levels increased 3-fold from 8 h to 30 h of starvation (*p* < 0.001).

KMCP1 expression was also examined *in vitro* in HK2 cells in response to nutrient deprivation. Cell starvation was accomplished by replacing the regular medium with a nutrient-poor medium. KMCP1 protein expression was induced progressively and significantly to reach a 2-fold level of increased expression upon 30 h of nutrient deprivation (*p* < 0.001)(Fig. 7D).

## DISCUSSION

**KMCP1 Is a Mitochondrial Carrier Expressed Mainly in the Kidney**—The phylogenetic tree in Fig. 1B clearly shows that this novel carrier belongs to the mitochondrial carrier family. Furthermore, the amino acid sequence of KMCP1 presents all of the known mitochondrial carrier signature motifs. KMCP1 RNA was detected in numerous tissues, with predominant expression in the kidney and testes. Our antibody raised against full-length KMCP1 specifically recognized the protein when expressed in yeast and mammalian cells, which allowed us to perform *in vivo* studies of this protein. At the tissue level, the KMCP1 protein is expressed in the kidney, and at the cellular level, it is expressed in mitochondria. The mammalian kidney is a complex organ, with its structural unit, the nephron, composed of several cell populations, each displaying

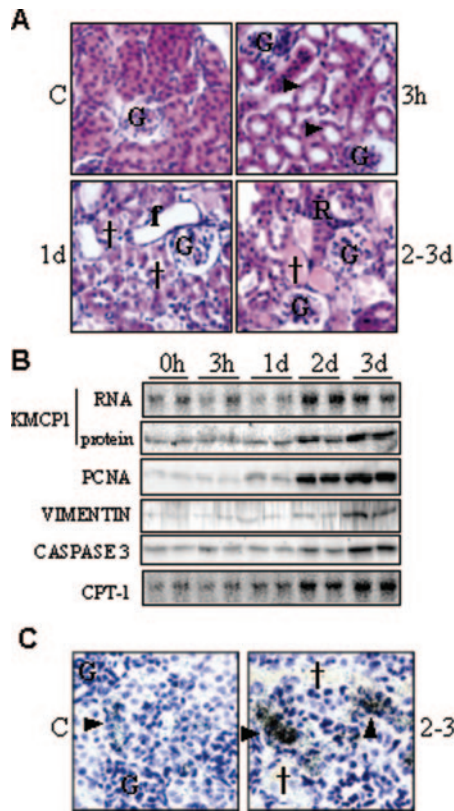


**FIG. 4. KMCP1 induction with glycerol-mediated renal failure.** A time course experiment was performed, and mouse kidneys were studied 3 h and 1, 2, and 3 days (*d*) after glycerol injection. Comparable sections and representative pictures of three experiments are presented from histology and *in situ* hybridization experiments. *A*, histological examinations of kidney cortex sections (magnification  $\times 400$ ). Sections were stained with hematoxylin and eosin. Glomeruli are indicated (*G*). Apical brush-border loss (indicated by arrowheads) was observed 3 h after glycerol injection (*upper right panel*). Tubular cell death ( $\dagger$ ) and distal cell flattening (*f*) were observed on day 1 (*lower left panel*). On days 2 and 3, completely necrosed ( $\ddagger$ ) or regenerated (*R*) tubular cells were present (*lower right panel*). *Upper left panel*, control (*C*). *n* > 3 in each group. *B*, Northern blot analysis of KMCP1 RNA (*first panel*) and Western blot analysis of the KMCP1 protein, PCNA, vimentin, and caspase-3 (*second through fifth panels*, respectively). KMCP1 was detected in renal mitochondria, whereas renal lysates were used for PCNA, vimentin, and caspase-3 analysis. Carnitine palmitoyltransferase-1 (*CPT-1*) was detected by Northern blot analysis (*n* > 4) (*sixth panel*). *C*, *in situ* experiment using the mouse KMCP1 cDNA antisense probe with kidney cortex sections. Glomeruli are indicated (*G*). Positive (*arrowheads*) and necrosed ( $\dagger$ ) cells are indicated. *Left panel*, kidney sections from control (*C*) mice; *right panel*, kidney sections from glycerol-injected mice.

diverse morphological, biochemical, and functional properties. As shown by *in situ* hybridization and immunochemistry studies, KMCP1 expression is restricted to the renal cortex and more precisely to proximal and distal tubules. These data are in accordance with quantitative real-time PCR results.

**KMCP1 Is Not Involved in Sodium and Water Homeostasis or in Glutamine Metabolism**—In an attempt to understand the physiological functions of KMCP, its expression was examined in a variety of animal models of perturbed renal function. Diuretics modify sodium reabsorption in different parts of the nephron. Changes in sodium transport are also observed during water deprivation as well as in animals fed a hypo- or hypernatremic diet or treated with cyclosporin A (19, 20). None of these situations examined in this study was associated with a significant change in KMCP1 levels.

In the kidney, glutamine metabolism is essential to maintain the systemic acid-base balance because it is the most important donor of ammonium ions. Increased renal ammoniogenesis

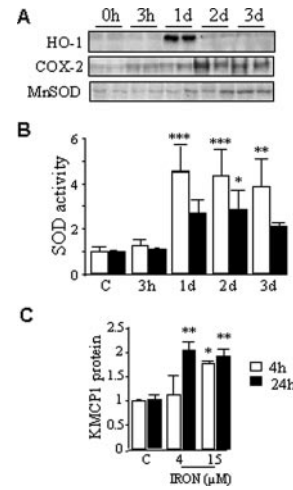


**FIG. 5. Cellular pathways involved in glycerol-mediated nephrotoxicity.** Mouse kidneys were studied before (control (*C* and *0h*)) and 3 h and 1, 2, and 3 days (*d*) after glycerol injection. *A*, Western blot analysis of cellular heme oxygenase-1 (*HO-1*), cyclooxygenase-2 (*COX-2*), and mitochondrial superoxide dismutase (*MnSOD*). Mitochondrial superoxide dismutase was detected in renal mitochondria, whereas renal lysates were used for detection of the other proteins (*n* = 4). *B*, superoxide dismutase activity in lysate (*white bars*) and mitochondria (*black bars*) isolated from mouse kidney (*n* = 4). *C*, KMCP1 protein expression in HK2 cells after treatment with iron. The results are means  $\pm$  S.E. (*n* = 4–6). \*, *p* < 0.05; \*\*, *p* < 0.01; \*\*\*, *p* < 0.001.

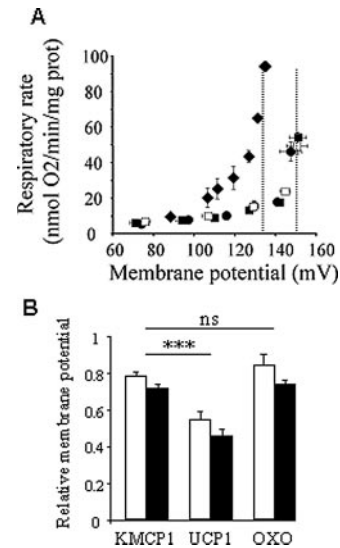


**FIG. 6. Functional analysis of mouse KMCP1.** *A*, relationship between the mitochondrial membrane potential and respiration rate in yeast transformed with the control vector ( $\square$ ) or expressing KMCP1 ( $\bullet$ ), the mitochondrial oxoglutarate carrier ( $\blacksquare$ ), or UCP1 ( $\blacklozenge$ ). These experiments were performed using the same amount of mitochondria in the presence of oligomycin and NADH. UCP1 expression increased proton leaking, whereas there was no difference in respiratory rate in yeast expressing KMCP1 or the oxoglutarate carrier. The results are means  $\pm$  S.E. from five independent experiments. *prot*, protein. *B*, flow cytometry analysis of the mitochondrial membrane potential using the tetramethylrhodamine ethyl ester probe in transiently transfected COS-7 cells with GFP and KMCP1, UCP1, or the oxoglutarate carrier (*OXO*). The results are presented as the ratio between the membrane potential of GFP-positive cells expressing the protein of interest and the membrane potential of GFP-negative cells in the absence (*white bars*) or presence (*black bars*) of oligomycin. The results are means  $\pm$  S.E. of 7–15 independent experiments. *ns*, not significant. \*\*\*, *p* < 0.001.

during metabolic acidosis constitutes an adaptive response that partially restores acid-base balance (21). KMCP1 expression did not change after induced metabolic acidosis. Taken together, these data argue against a role for KMCP1 in sodium and water homeostasis or in glutamine metabolism.

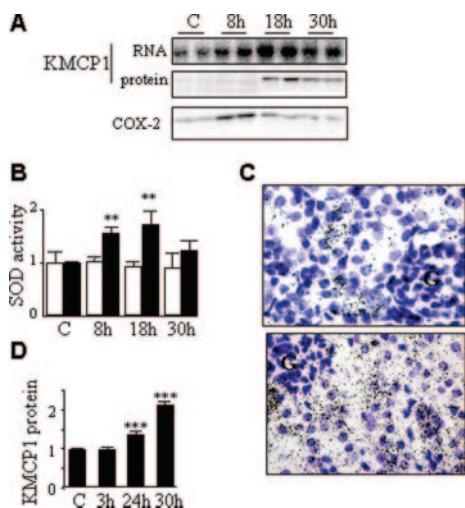


**FIG. 7. Induction of KMCP1 during fasting.** A time course experiment was performed, and mouse kidneys were studied before (control (C)) and at 8, 18, and 30 h during starvation. Comparable sections and representative pictures of three experiments are presented from *in situ* hybridization experiments. A, KMCP1 expression. Northern blotting was performed with total RNA (20  $\mu$ g) isolated from mouse kidney using  $^{32}$ P-labeled mouse KMCP1 cDNA ( $n = 11$ ). Western blot analysis of KMCP1 and cyclooxygenase-2 (COX-2) was performed using 15  $\mu$ g of renal proteins from mitochondria and lysate, respectively ( $n = 4-9$ ). B, superoxide dismutase (SOD) activity in lysate (white bars) and mitochondria (black bars) isolated from mouse kidney. The results are means  $\pm$  S.E. ( $n > 3$ ). C, *in situ* experiment using the mouse KMCP1 cDNA antisense probe with kidney cortex sections. Glomeruli are indicated (G). Left panel, kidney sections from control mice; right panel, kidney sections from fasting mice. D, KMCP1 protein in HK2 cells during starvation. The results are means  $\pm$  S.E. ( $n = 4-6$ ). \*\*,  $p < 0.01$ ; \*\*\*,  $p < 0.001$ .

**KMCP1 Levels Increase during Cell Proliferation**—In humans, a common cause of acute renal failure is acute tubular necrosis, in which damage to the tubular epithelium occurs in response to renal ischemia or drug or toxin exposure. Studies on drug-induced models of acute tubular necrosis suggest that the first stage of the nephrotoxicity process occurs in the proximal tubules, later progressing to tubular necrosis and apoptosis. After such an injury, the kidney has the ability to partially recover function through repairing its tubular epithelium. This recovery phase includes cell dedifferentiation and proliferation to restore cell number, followed by redifferentiation, which ultimately results in the restoration of the structural and functional integrity of the tubular epithelium (22). In our mouse model of glycerol-mediated renal failure, all of these processes were observed sequentially: only hours after the myoglobinuric state induced by glycerol injection (23), acute renal failure occurred as reflected by rising blood urea nitrogen and creatinine levels. Interestingly, histological examination of kidney sections and caspase-3 levels as well as TUNEL experiments showed apoptosis and necrosis occurring predominantly in renal proximal tubular cells only a few hours after glycerol challenge. During this stage, KMCP1 levels did not change, suggesting that KMCP1 is not involved in cell death. However, in the days following glycerol injection, during which histological examination showed tubular regeneration and maximal PCNA immunoreactivity, the KMCP1 level was significantly up-regulated. Moreover, KMCP1 expression was induced specifically in proximal tubules, where the injury was the most marked. These observations suggest that KMCP1 plays some role in the regenerative capability of the tubular epithelium following injury.

Tubular regeneration following glycerol-induced injury is associated with increased mitochondrial  $\beta$ -oxidation and protein catabolism as indicated by carnitine palmitoyltransferase-1

and blood urea nitrogen levels, respectively. During starvation, the energy required to maintain physiological function derives from the oxidation of lipids and proteins because glycogen stores are exhausted rapidly during starvation. Thus, one potential mechanism explaining the up-regulation of KMCP1 in response to tubular regeneration and fasting is that KMCP1 might achieve a shift in cellular substrate utilization from carbohydrate to lipid metabolism.

**KMCP1 Expression Increases in Response to Oxidative Damage**—Hypertonic glycerol injection is the most widely used model for myoglobinuric acute renal failure. Whether the precise mechanism is due to free iron, free heme, or free radicals is still debated. Free heme molecules are cytotoxic and lead eventually to cell death. Although heme oxygenase-1, the rate-limiting enzyme in heme metabolism, effectively removes the heme molecules, the conversion of the heme ring to biliverdin results in iron release. Free iron can then promote free radical formation via the Haber-Weiss reaction, leading to cellular oxidative stress. In this model, up-regulation of KMCP1 expression follows heme oxygenase-1 activation. Cyclooxygenase-2 is another pro-inflammatory enzyme because superoxide anion is produced as a by-product of its enzymatic action. Interestingly, cyclooxygenase-2 increases in the glycerol-mediated failure model and during fasting, another physiological situation characterized by increased KMCP1 expression. These results suggest that KMCP1 could be up-regulated in response to the oxidative stress generated by these enzymes. This hypothesis is supported by the fact that, in both models, KMCP1 up-regulation occurs simultaneously with increased antioxidant enzymes (superoxide dismutase). Furthermore, KMCP1 expression increases in the gentamicin- and cisplatin-induced mouse models of renal failure. Gentamicin, an aminoglycoside antibiotic, has been shown to enhance generation of superoxide anion and hydrogen peroxide by renal cortex mitochondria (24, 25). Cisplatin, a widely used antineoplastic agent, has nephrotoxicity as a major side effect, which occurs through reactive oxygen species production (26). Finally, expression of KMCP1 is directly up-regulated by iron *in vitro*.

In conclusion, this study has presented the characterization of a new mitochondrial carrier protein, KMCP1. This carrier is expressed specifically in the kidney and is up-regulated during fasting and the regenerative phase following renal tubular injury. We suggest that its role may involve a shift from carbohydrate to lipid metabolism and/or protection from oxidative damage in situations of increased mitochondrial metabolism. A vast majority of research in the field of acute renal failure has focused on the determination of events and factors that cause renal proximal tubular cell injury and death. However, the responses of surviving proximal tubules are also crucial to the restoration of renal function. Consequently, studying KMCP1 could help in understanding mechanisms underlying kidney repair and regeneration mechanisms.

**Acknowledgments**—We are grateful to Alain Doucet for work in quantitative real-time PCR, Gérard Pivert for histology, Corinne Antignac and Marie-Claire Gubler for discussions, and Nathan Hellman for critical reading of the manuscript.

#### REFERENCES

1. Palmieri, F. (2004) *Pfluegers Arch.* **447**, 689–709
2. Pebay-Peyroula, E., Dahout-Gonzalez, C., Kahn, R., Trezeguet, V., Lauquin, G. J., and Brandolin, G. (2003) *Nature* **426**, 39–44
3. Sanchis, D., Fleury, C., Chomiki, N., Goubern, M., Huang, Q., Neverova, M., Gregoire, F., Easlick, J., Raimbault, S., Levi-Meyrueis, C., Miroux, B., Collins, S., Seldin, M., Richard, D., Warden, C., Bouillaud, F., and Ricquier, D. (1998) *J. Biol. Chem.* **273**, 34611–34615
4. Kondou, S., Hidaka, S., Yoshimatsu, H., Tsuruta, Y., Itateyama, E., and Sakata, T. (2000) *Biochim. Biophys. Acta* **1457**, 182–189
5. Kim-Han, J. S., Reichert, S. A., Quick, K. L., and Dugan, L. L. (2001) *J. Neurochem.* **79**, 658–668
6. Yu, X. X., Mao, W., Zhong, A., Schow, P., Brush, J., Sherwood, S. W., Adams, S. H., and Pan, G. (2000) *FASEB J.* **14**, 1611–1618

7. Yang, X., Pratley, R. E., Tokraks, S., Tataranni, P. A., and Permana, P. A. (2002) *Mol. Genet. Metab.* **75**, 369–373
8. Sullivan, P. G., Rippey, N. A., Dorenbos, K., Concepcion, R. C., Agarwal, A. K., and Rho, J. M. (2004) *Ann. Neurol.* **55**, 576–580
9. Mizuno, T., Miura-Suzuki, T., Yamashita, H., and Mori, N. (2000) *Biochem. Biophys. Res. Commun.* **278**, 691–697
10. Lengacher, S., Magistretti, P. J., and Pellerin, L. (2004) *J. Cereb. Blood Flow Metab.* **24**, 780–788
11. Pecqueur, C., Alves-Guerra, M.-C., Gelly, C., Levi-Meyrueis, C., Couplan, E., Collins, S., Ricquier, D., Bouillaud, F., and Miroux, B. (2001) *J. Biol. Chem.* **276**, 8705–8712
12. Miroux, B., and Walker, J. E. (1996) *J. Mol. Biol.* **260**, 289–298
13. Harlow, E., and Lane, D. (1988) *Antibodies: A Laboratory Manual*, Cold Spring Harbor Laboratory, Cold Spring Harbor, NY
14. Cassard, A. M., Bouillaud, F., Mattei, M. G., Hentz, E., Raimbault, S., Thomas, M., and Ricquier, D. (1990) *J. Cell. Biochem.* **43**, 255–264
15. Gonzalez-Barroso, M. M., Fleury, C., Arechaga, I., Zaragoza, P., Levi-Meyrueis, C., Raimbault, S., Ricquier, D., Bouillaud, F., and Rial, E. (1996) *Eur. J. Biochem.* **239**, 445–450
16. González-Barroso, M. M., Fleury, C., Bouillaud, F., Nicholls, D. G., and Rial, E. (1998) *J. Biol. Chem.* **273**, 15528–15532
17. Chabardès-Garonne, D., Mejean, A., Aude, J. C., Cheval, L., Di Stefano, A., Gaillard, M. C., Imbert-Teboul, M., Wittner, M., Balian, C., Anthonard, V., Robert, C., Segurens, B., Wincker, P., Weissenbach, J., Doucet, A., and Elalouf, J. M. (2003) *Proc. Natl. Acad. Sci. U. S. A.* **100**, 13710–13715
18. Halliwell, B., and Gutteridge, J. M. (1990) *Methods Enzymol.* **186**, 1–85
19. Faulds, D., Goa, K. L., and Benfield, P. (1993) *Drugs* **45**, 953–1040
20. Brewster, U. C., and Perazella, M. A. (2004) *Am. J. Med.* **116**, 263–272
21. Curthoys, N. P. (2001) *J. Nutr.* **131**, 2491S–2495S; Discussion (2001) *J. Nutr.* **131**, 2496S–2497S
22. Thadhani, R., Pascual, M., and Bonventre, J. V. (1996) *N. Engl. J. Med.* **334**, 1448–1460
23. Thiel, G., Wilson, D. R., Arce, M. L., and Oken, D. E. (1967) *Nephron* **4**, 276–297
24. Ali, B. H. (2003) *Food Chem. Toxicol.* **41**, 1447–1452
25. Walker, P. D., Barri, Y., and Shah, S. V. (1999) *Renal Fail.* **21**, 433–442
26. Baliga, R., Zhang, Z., Baliga, M., Ueda, N., and Shah, S. V. (1998) *Kidney Int.* **53**, 394–401
27. Miroux, B., Frossard, V., Raimbault, S., Ricquier, D., and Bouillaud, F. (1993) *EMBO J.* **12**, 3739–3745